JOURNAL OF CATALYSIS **167,** 425–437 (1997)
ARTICLE NO. CA971594

Neopentane Conversion over Zeolite-Supported Platinum and Palladium Catalysts

Paul V. Menacherry and Gary L. Haller

Department of Chemical Engineering, Yale University, 9 Hillhouse Avenue, New Haven, Connecticut 06520

Received March 26, 1996; revised November 21, 1996; accepted December 20, 1996

Neopentane conversion has been studied over platinum supported on L- and Y-zeolites, and palladium supported on KL-zeolite. The Pd/KL-zeolite catalysts exhibit the enhanced activation energies previously reported in the literature. The preexponential factors and activation energies show a compensation effect for both the palladium and the platinum catalysts. The trend in activation energies is compared with hydrogen TPD studies. Pressure dependence studies (in excess hydrogen) show reaction orders of approximately −2 and 0.8 for hydrogen and neopentane, respectively, except for hydrogenolysis over Pd/KL which exhibits reaction orders of ∼−4 and 0.64, respectively. At lower hydrogen pressures (<70 Torr) the reaction order in hydrogen becomes less negative, which may signify a change in the rate-limiting step of the reaction. The nature of the adsorbed intermediates, probable reaction pathways, and the compensation effect are discussed.

INTRODUCTION

Platinum and palladium supported on zeolites have been the focus of considerable research. Both steric effects of the zeolite supports (1) and metal support interaction effects (2–7) have been observed for reactions over these catalysts. The metal support interaction can be varied by changing the Brønsted acidity (2–4) and/or the charge-compensating cations of the zeolite support (5–7) and may manifest itself as an electronic perturbation of the metal particles. Thus both electron-deficient (5, 8) and electron-rich (9) metal particles have been reported.

The reaction of neopentane with hydrogen can be a valuable probe of metal support interaction, because the inability of this molecule to form olefins as primary products confines the reaction to the metal sites under differential conditions (5). Foger and Anderson (5) observed a decrease in the activation energies for neopentane conversion over different Pt/Y-zeolite catalysts with increased electron deficiency. A similar trend was reported by Bai *et al.* (6) over different Pd/Y-zeolite catalysts. Modica *et al.* studied the activity for neopentane conversion over KL-zeolite-supported platinum (3) and palladium (4) modified by introducing Brønsted acidity/excess cation basicity, and found that the activity increased with the acidity of the support. Hence neopentane conversion can be used to probe metal support interaction in supported platinum and palladium catalysts.

Recently, Karpinski *et al.* (7) reported enhanced activation energies (∼78–90 kcal/mol) for neopentane conversion over palladium supported on L-zeolite relative to palladium supported on silica or alumina. They postulated that this may be due to single-file diffusion in the L-zeolite pores. However, platinum on L-zeolite does not exhibit these enhanced activation energies (10). Therefore, it seemed unlikely that the enhanced activation energies were due to diffusion effects. In the present work, the kinetic and partial pressure dependence for neopentane conversion over different Pt/L-, Pt/KY-, and Pd/KL-zeolite catalysts have been studied, and the results have been correlated with the Temperature Programmed Desorption (TPD) of hydrogen over these catalysts. The effect of partially exchanging the cations present in the locked cages, and of varying the Brønsted acidity, has been studied for platinum supported on L-zeolite, and these have been compared with Pt/KY and Pd/KL-zeolites of different Brønsted acidities.

EXPERIMENTAL

Catalyst Preparation

The KL-zeolite and NaY-zeolite (SiO_2/Al_2O_3 ratio = 3) were obtained from TOSOH. A partial cation exchange of the KL-zeolite was carried out to exchange the cations present in the locked sites (11). Portions of the KL-zeolite were slurried in 250 ml/g of 0.4 *N* solutions of $Ca(NO_3)_2$, $Ba(NO_3)_2$, and $La(NO_3)_3$, respectively, for 24 h. The samples were filtered using a Büchner funnel, and dried at 140°C for 18 h. They were then heated to 500°C at 2°C/min and calcined at this temperature for 3 h in 7.2 liters/min flow of oxygen. The calcined samples were then subjected to a back-exchange using a 0.4 *N* solution of KNO_3, filtered, and dried at 140°C for 18 h. These supports are denoted as CaKL, BaKL, and LaKL, respectively. The KL-zeolite was also used as received.

Platinum (5.5 wt%) was introduced on these four supports by ion-exchange using the tetraamine platinum

0021-9517/97 $25.00

nitrate precursor. Portions of the support were slurried in 200 ml/(g of support) deionized water and a solution of the precursor in 100 ml of deionized water was added dropwise over 2 h. The ion-exchange was carried out over 24 h. The samples were filtered, then dried at 140°C for 18 h. They were then heated to 300°C at 2°C/min and calcined at this temperature for 2 h in 600 ml/(min × g of catalyst) flow of oxygen, cooled to room temperature in 400 ml/(min × g of catalyst) flow of helium, then heated to 400°C, reduced at this temperature for 1 h, and cooled to room temperature, in 400 ml/(min × g of catalyst) flow of hydrogen. The samples were then passivated in air and stored.

The KY-zeolite was prepared from NaY-zeolite by ion exchange using a 0.4 *N* solution of KNO_3. Platinum (3.67 wt%) supported on KL-zeolite and KY-zeolite and palladium (2 and 3 wt%) supported on KL-zeolite were prepared using tetraamine platinum nitrate and tetraamine palladium nitrate as precursors, using the above procedure. Portions of the Pt/KL (3.67 wt%), Pt/KY (3.67 wt%), and Pd/KL (2.0 wt%) were subject to a back-exchange (BE) with K^+ to remove protons generated in the reduction step. Portions of these catalysts were slurried in a solution of KOH in 200 ml/(g of catalyst) deionized water for 24 h, with the pH maintained between 8.5 and 9.0 by the addition of KOH. The samples were filtered, and then dried at 140°C for 24 h.

Chemisorption

Chemisorption experiments were performed in a conventional static adsorption apparatus described elsewhere (12). A 400-mg portion of catalyst was heated to 400°C and rereduced at this temperature for 30 min in 160 ml/min flow of hydrogen. The flow was then switched to helium (160 ml/min), and the sample was purged at this temperature for 30 min to remove chemisorbed hydrogen, and then cooled to room temperature. Hydrogen uptake was measured for equilibrium pressures in the range 10 to 150 Torr. The sample was then exposed to 760 Torr of hydrogen for 20 min and evacuated for 1 h, and then the uptake of oxygen was measured in the same range of equilibrium pressures. The oxygen uptake (O/M) was calculated by subtracting half the hydrogen uptake (H/M) extrapolated to zero pressure from the total uptake of oxygen.

TPD of Hydrogen

Temperature-programmed desorptions of hydrogen were carried out in a packed bed configuration using 7-mm-i.d. Pyrex tube reactors. The catalyst bed consisted of 100 mg of catalyst diluted in 500 mg of α-alumina. The hydrogen, carrier nitrogen, and reference nitrogen gas flows were controlled using mass flow controllers. Nitrogen was purified upstream of the catalyst bed using an Oxiclear purifying trap (Labclear) and an OMI-2 indicating purifier trap (Supelco, Inc.). Hydrogen was purified upstream of the catalyst bed using an Oxiclear purifying trap and a liquid nitrogen trap. The effluent from the catalyst bed was passed through a dry ice acetone trap before entering the thermal conductivity detector (TCD).

The samples were rereduced at 400°C and then allowed to cool slowly to room temperature, in a flow of 10 ml/min hydrogen and 30 ml/min nitrogen. The hydrogen flow was then switched off and the reactor was purged in the nitrogen (carrier) flow until a stable baseline was reached in the TCD (∼1 h). A temperature ramp of 6°C/min to 400°C was used and the desorptions were monitored using the TCD. The X–Y data were smoothed using a Savitzky–Golay algorithm (13) of fourth order ($N_R = N_L = 3$) and then numerically differentiated to determine peak positions.

Neopentane Reaction

A 10% neopentane blend in helium was obtained from Scott Specialty Gases. This was further purified by being passed through a commercial OMI-2 indicating purifier trap (Supelco, Inc.) and a 5 Å molecular sieve trap. The neopentane conversion was carried out in a 10-mm-i.d. Pyrex tube packed-bed-type reactor operated at near atmospheric pressure. The catalyst bed consisted of 200 mg of sample diluted in 1 g of α-alumina. The inlet feed streams were mixed and then preheated in an α-alumina bed before flowing through the catalyst bed. The samples were rereduced at 400°C for 30 min (under the hydrogen and balance helium gas flows) and cooled to the initial reaction temperature, and then the neopentane blend was introduced. The reaction products were analyzed by an on-line Varian 3700 GC equipped with a packed column and a flame ionization detector. The temperature dependence of the reaction over the different catalysts was probed over a range of 30°C. The balance gas was then switched to nitrogen and the temperature dependence of the reaction was again probed. The gas flows used were 10 ml/min hydrogen, 10 ml/min neopentane blend, and 80 ml/min balance gas. The partial pressures of neopentane and hydrogen in these studies were 1.0 and 10.4 kPa, respectively. The level of conversion was less than 4% for the studies on all of the platinum catalysts. Because of the higher activation energies over the palladium catalysts, slightly higher conversions were used over these catalysts. The level of conversion at the highest temperatures used in these studies were 7.4, 8.0, and 13.2% for the 2.0 wt%, the 2.0 wt% back-exchanged, and the 3.0 wt% Pd/KL samples, respectively. The α-alumina displayed no activity for neopentane conversion at the reaction temperatures used.

The kinetic pressure dependence of the reaction rate was studied over three catalysts, Pt/KL (3.67 wt%, BE), Pt/KY (3.67 wt%, BE), and Pd/KL (2.0 wt%). The temperature of reaction was held constant and catalytic activity was measured 20 and 40 min after changing the partial pressures, to check for steady state/deactivation.

TABLE 1

Hydrogen Chemisorption and Oxygen Reverse Titration

Catalyst	H/M chemisorption	O/M	H/M (TPD)
Pt/KL (5.5 wt%)	1.12	0.34	0.94
Pt/CaKL (5.5 wt%)	1.14	0.32	0.98
Pt/BaKL (5.5 wt%)	1.19	0.30	1.22
Pt/LaKL (5.5 wt%)	1.17	0.30	1.06
Pt/KL (3.67 wt%)	1.71	0.50	1.86
Pt/KL (3.67 wt%, BE)	1.61	0.53	1.62
Pt/KY (3.67 wt%)	1.34	0.43	1.11
Pt/KY (3.67 wt%, BE)	1.14	0.49	0.92
Pd/KL (3.0 wt%)	0.72	0.33	0.34
Pd/KL (2.0 wt%)	0.58	0.36	0.49
Pd/KL (2.0 wt%, BE)	0.60	0.39	0.58

TABLE 2

TPD of Hydrogen

Catalyst	Hydrogen TPD peak positions (°C)			
	Peak I	Peak II	Peak III	Peak IV
Pt/KL (5.5 wt%)	96	144	—	—
Pt/CaKL (5.5 wt%)	92	154	—	—
Pt/BaKL (5.5 wt%)	90	150	—	—
Pt/LaKL (5.5 wt%)	90	156	—	—
Pt/KL (3.67 wt%)	102	192	—	—
Pt/KL (3.67 wt%, BE)	90	174	192	
Pt/KY (3.67 wt%)	78	150	276	
Pt/KY (3.67 wt%, BE)	78	150	210	300
Pd/KL (3.0 wt%)	78	126	222	—
Pd/KL (2.0 wt%)	78	144	252	—
Pd/KL (2.0 wt%, BE)	90	168	240	312

RESULTS

Chemisorption

The hydrogen and oxygen uptakes extrapolated to zero pressure are reported in Table 1. It is seen that all the platinum catalysts are highly dispersed (H/Pt > 1). A comparison of the hydrogen and oxygen uptakes for the 5.5 wt% Pt series shows that these catalysts have very similar dispersion. We observe that for platinum, back-exchange of the protons generated upon reduction results in a smaller hydrogen uptake while for palladium the back exchange results in a larger hydrogen uptake. This point will be discussed in the context of the electronic modification of the metal particles in these catalysts. Although the hydrogen uptake on the palladium catalysts is less than one, EXAFS of these samples suggest that these are highly dispersed. The first shell coordination numbers determined from EXAFS are 3.4 and 4.4 for the low and high loading samples, respectively (14), while these are between 5 and 6 for the platinum samples (15).

TPD of Hydrogen

The TPD of hydrogen over the different catalysts is shown in Figs. 1, 2, 3, and 4. The integrated peak areas are reported in Table 1 and the peak positions are reported in Table 2. The hydrogen desorption temperatures for the 5.5 wt% Pt/L-zeolites are similar; however, a qualitative trend (because of possible particle size

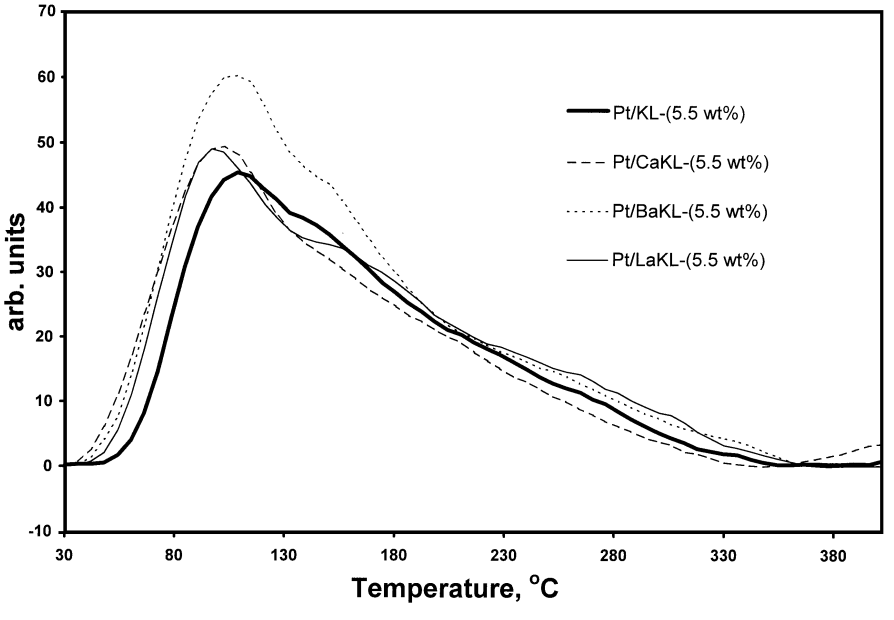

FIG. 1. TPD of hydrogen (5.5 wt% Pt/L-zeolite).

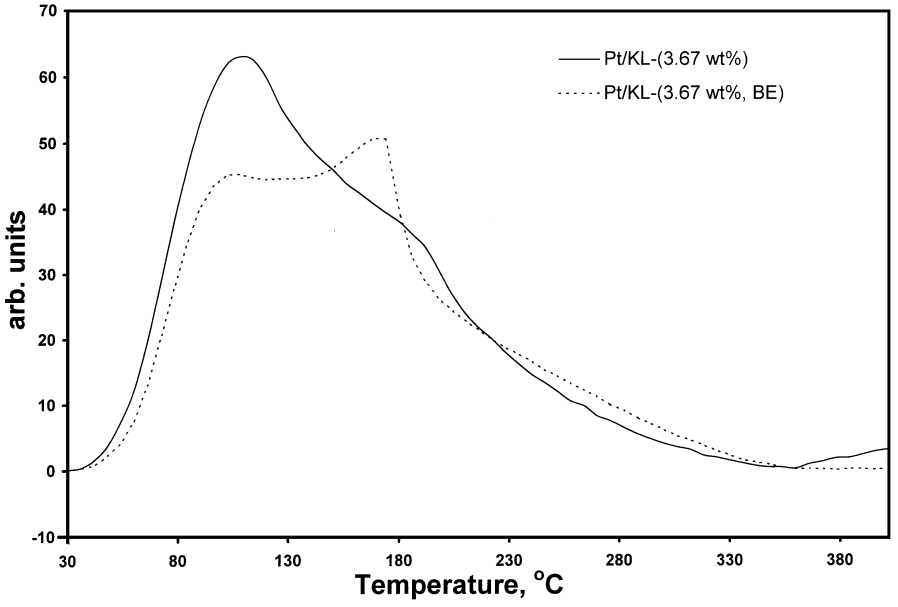

FIG. 2. TPD of hydrogen (3.67 wt% Pt/L-zeolite).

effects) in the amount of hydrogen desorbed can be observed. A comparison of the TPD of hydrogen for the ion-exchanged and back-exchanged samples of Pt/KL-zeolite and Pt/KY-zeolite shows that back-exchange results in higher binding states for hydrogen with a decrease in the total hydrogen adsorbed. The opposite trend is observed for Pd/KL-zeolite. These trends in the TPD of hydrogen have been correlated with the activation energies for neopentane conversion over these catalysts (see below).

Neopentane Reaction

Deactivation of the catalysts was negligible under the conditions of the temperature dependence studies. The observed reaction products were methane, ethane, propane, isobutane, *n*-butane, and isopentane. Mojet *et al.* (4) concluded from the analysis of the reaction products by the Delpot method (16) that the primary reaction products are methane and isobutane (hydrogenolysis) and isopentane (isomerization). A similar conclusion was reached by

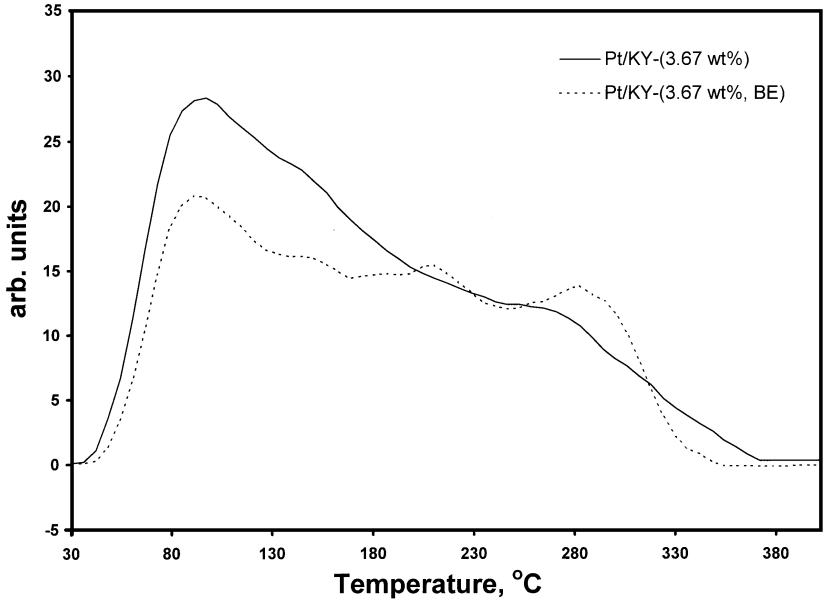

FIG. 3. TPD of hydrogen (3.67 wt% Pt/Y-zeolite).

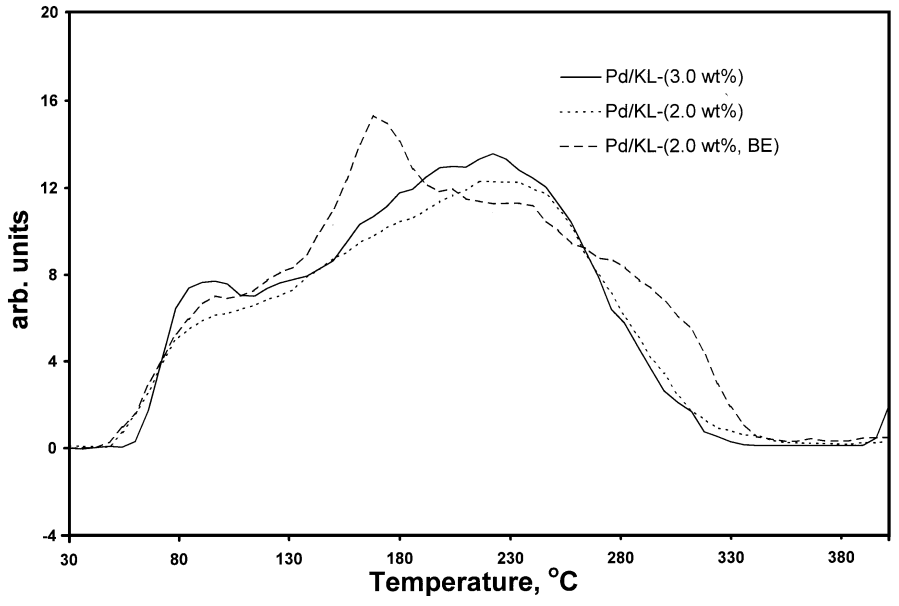

FIG. 4. TPD of hydrogen (Pd/L-zeolite).

Karpinski *et al.* (7). We have assumed the following reaction sequence in order to analyze the reaction products:

$$\begin{array}{l} \text{neopentane} \rightarrow i\text{-pentane} \rightarrow n\text{-butane} + \text{methane} \\ \qquad\qquad\quad \downarrow \\ \qquad i\text{-butane} + \text{methane} \\ \qquad\qquad\quad \downarrow \\ \qquad \text{propane} + \text{methane} \\ \qquad\qquad\quad \downarrow \\ \qquad \text{ethane} + \text{methane}. \end{array}$$

This implies that the moles of neopentane undergoing hydrogenolysis is equal to the sum of the moles of *i*-butane, propane, and ethane produced, and the moles of neopentane undergoing isomerization is equal to the sum of the moles of *i*-pentane and *n*-butane produced. The assumption that all of the propane and ethane is formed from isobutane is quite valid, because these products appear only at higher conversions where isobutane concentration is about two orders of magnitude larger than the *n*-butane concentration.

Turnover frequencies were obtained by normalizing to the hydrogen uptake values given in Table 1, for the platinum samples. For the palladium samples, the rates were normalized to the integrated peak areas from the hydrogen TPD (also given in Table 1), because EXAFS of the high loading sample under hydrogen atmosphere (14) showed lattice expansion indicating bulk hydride formation. It was observed that the hydrogenolysis and isomerization reactions could be modeled independently by Arrhenius type parameters. The Arrhenius plots are shown in Fig 5. The activation energies and preexponential factors are reported in Table 3. Changing the balance gas from helium to nitrogen

TABLE 3

Kinetic Parameters

Catalyst	Temp. range (°C)	TOF (total) range (sec^{-1})	Activation energy (kcal/mol)		Preexponential factor	
			Hydrogenolysis	Isomerization	Hydrogenolysis	Isomerization
Pt/KL (5.5 wt%)	170–200	4.1E-5–3.1E-4	28.5 ± 1.0	29.3 ± 1.4	4.07E+09	1.30E+09
Pt/CaKL (5.5 wt%)	170–200	5.6E-5–3.2E-4	24.5 ± 1.6	27.2 ± 1.9	6.11E+07	1.54E+08
Pt/BaKL (5.5 wt%)	170–200	6.2E-5–3.3E-4	23.4 ± 1.7	25.5 ± 1.5	1.79E+07	2.26E+07
Pt/LaKL (5.5 wt%)	170–200	3.6E-5–2.8E-4	27.0 ± 0.9	30.3 ± 0.8	7.36E+08	2.57E+09
Pt/KL (3.67 wt%)	170–200	3.6E-5–2.8E-4	28.9 ± 1.2	29.9 ± 1.3	5.43E+09	2.19E+09
Pt/KL (3.67 wt%, BE)	190–220	4.2E-5–4.5E-4	37.2 ± 1.3	33.1 ± 1.9	1.23E+13	2.10E+10
Pt/KY (3.67 wt%)	200–230	3.2E-5–5.0E-4	44.2 ± 0.7	39.5 ± 0.8	5.53E+15	2.33E+13
Pt/KY (3.67 wt%, BE)	230–260	4.2E-5–6.9E-4	52.6 ± 1.2	44.9 ± 1.1	1.99E+18	4.65E+14
Pd/KL (3.0 wt%)	230–260	2.5E-5–2.4E-3	80.2 ± 1.1	52.5 ± 4.2	1.61E+30	1.82E+17
Pd/KL (2.0 wt%)	230–260	3.3E-5–2.5E-3	78.2 ± 1.6	50.5 ± 3.8	2.46E+29	4.29E+16
Pd/KL (2.0 wt%, BE)	250–280	5.2E-5–2.3E-3	75.0 ± 1.5	44.1 ± 1.5	8.94E+26	2.28E+13

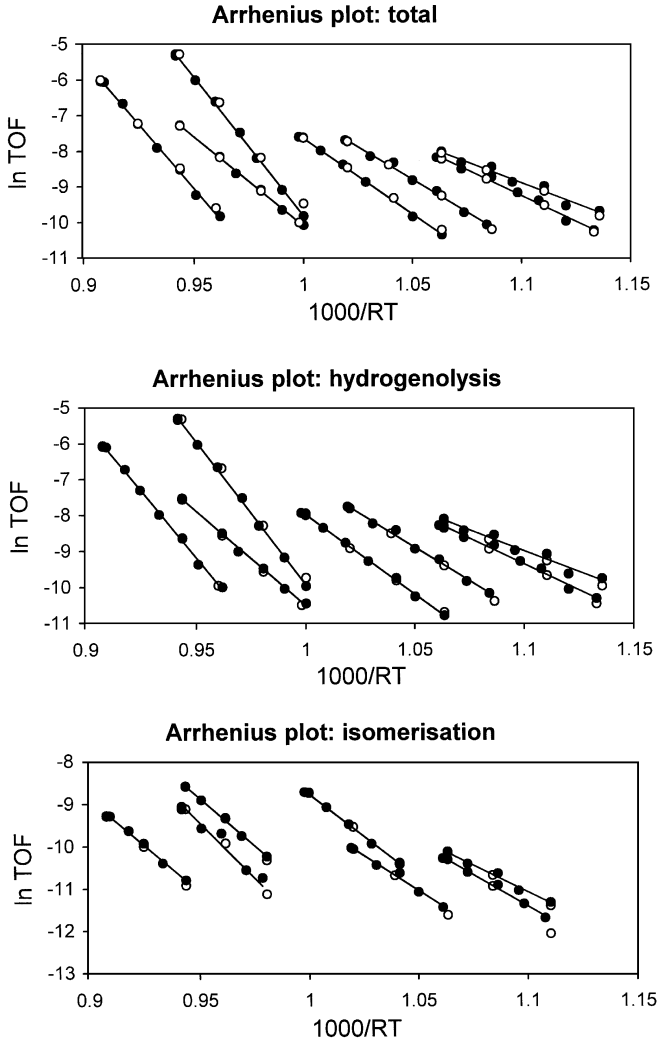

FIG. 5. Arrhenius plots (●), balance gas helium (○), balance gas nitrogen. [For total and hydrogenolysis, from left to right: Pd/KL (2.0 wt%, BE), Pt/KY (3.67 wt%, BE), Pd/KL (3.0 wt%), Pt/KY (3.67 wt%), Pt/KL (3.67 wt%, BE), Pt/KL (3.67 wt%), Pt/BaKL-(5.5 wt%); for isomerization: Pt/KY (3.67 wt%) and Pd/KL-(3.0 wt%) are interchanged in above ordering.]

had no effect on the activity of the catalysts as can be seen from the Arrhenius plots. The isomerization selectivity is observed to be a function of the reaction temperature, because of the different activation energies for isomerization and hydrogenolysis.

A compensation effect was observed in both hydrogenolysis and isomerization reactions. This is shown in Fig 6. The (apparent) activation energies for both hydrogenolysis and isomerization follow the same trend, i.e., Pt/BaKL (5.5 wt%) < Pt/CaKL (5.5 wt%) < Pt/LaKL (5.5 wt%) ≈ Pt/KL (5.5 wt%) ≈ Pt/KL (3.67 wt%) < Pt/KL (3.67 wt%, BE) < Pt/KY (3.67 wt%) < Pt/KY (3.67 wt%, BE), and Pd/KL (2.0 wt%, BE) < Pd/KL (2.0 wt%) < Pd/KL (3.0 wt%). Pd/L-zeolites show the opposite trend of Pt/L-zeolites in the variation of activation energies with Brønsted acidity. Karpinski *et al.* (7) have reported activation of energies of 77.7 and 81.1 kcal/mol for Pd/KL-zeolite and Pd/CaKL-zeolite, respectively, which is in agreement with this observation. The isokinetic temperatures were calculated from the compensation plots to be 300 and 298°C for the platinum samples, and 43 and 163°C for the Pd/KL-zeolite samples, for the hydrogenolysis and isomerization reactions, respectively.

The kinetic pressure dependence of the reaction rate over Pt/KL (3.67 wt%, BE), Pt/KY (3.67 wt%, BE) and Pd/KL (2.0 wt%) is shown in Fig. 7. The reaction orders for partial pressures of hydrogen (calculated for excess hydrogen, i.e., $P_{H_2} \geq 10.4$ kPa) and neopentane are reported in Table 4.

DISCUSSION

Diffusion Considerations

There are three indications that the rate-limiting step of neopentane conversion, under the conditions of the temperature dependence studies, is not the diffusion of reactants in the zeolite pores. First, the Koros-Nowak criterion (17) is satisfied by the two different loadings of platinum and palladium on KL-zeolite (before back exchange). Second, there is no effect of changing the balance gas from helium to nitrogen on catalytic activity, which might be expected to be affected in a manner similar to binary diffusion if the reaction were transport limited (18). Third, the neopentane conversion shows reaction orders close to unity in the partial pressure of neopentane. Therefore, we take as a working hypothesis that the neopentane conversion is not diffusion controlled, and seek an alternate explanation for the large difference in activation energies and the different response

TABLE 4

Reactant Pressure Dependence

Catalyst	Reaction temp. (°C)	Hydrogenolysis		Isomerization	
		Exponent for P_{neop}	Exponent for P_{H_2}	Exponent for P_{neop}	Exponent for P_{H_2}
Pt/KL (3.67 wt%, BE)	205	0.77 ± 0.05	-2.12 ± 0.1	0.81 ± 0.08	-2.23 ± 0.6
Pd/KL (2.0 wt%)	250	0.65 ± 0.03	-3.99 ± 0.3	0.78 ± 0.07	-1.92 ± 0.2
Pt/KY (3.67 wt%, BE)	250	0.92 ± 0.02	-2.59 ± 0.2	0.89 ± 0.03	-2.49 ± 0.2

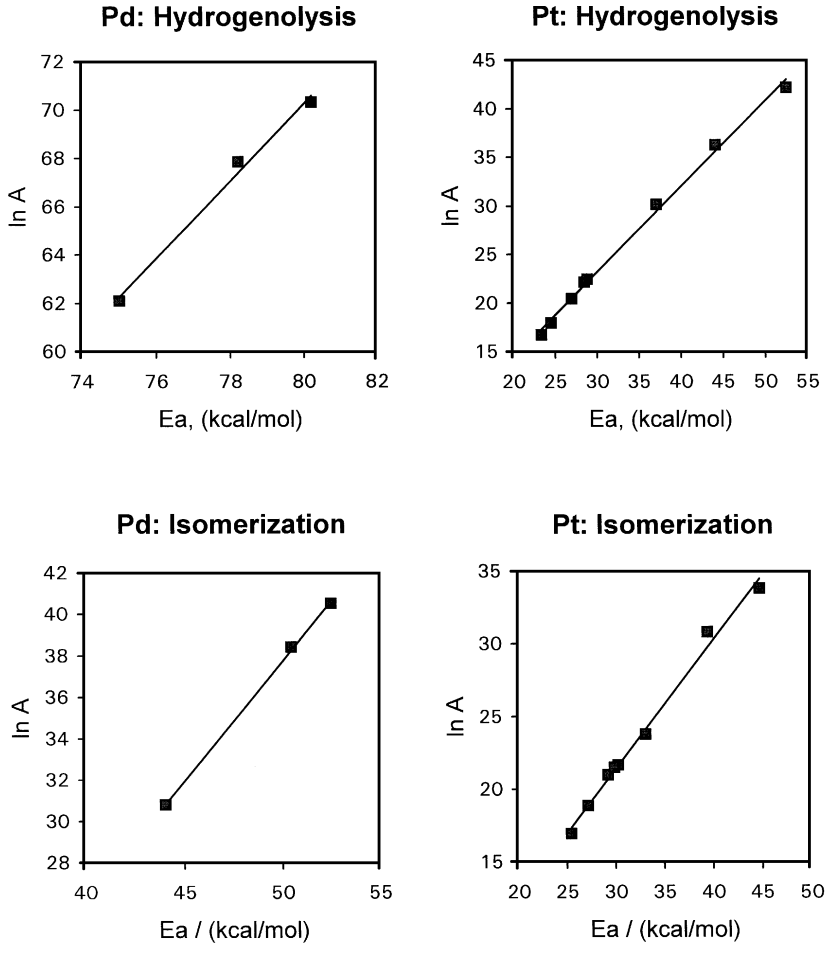

FIG. 6. Compensation effect.

to changes in acidity for platinum and palladium supported on L-zeolite.

The enhanced activation energies for neopentane conversion over Pd/L-zeolite catalysts was attributed previously (7) to a single-file diffusion effect (19). This assumes that under reaction conditions, the pores of the L-zeolite are plugged with neopentane (and product) molecules, and the enhanced activation energies reflect the greater mobility of the reactant molecules at higher temperatures. The length of the channel (from the pore mouth) where exchange with the gas phase occurs easily increases with temperature, because of decreased physisorption and increased mobility of the molecules, resulting in an increase in the apparent activation energy. However, the positive reaction orders in neopentane partial pressure observed, for neopentane conversion over these catalysts, are not consistent with this possibility. Figure 8 plots the selectivity toward secondary and tertiary hydrogenolysis (calculated as the sum of the moles of *n*-butane, propane, and ethane, divided by the sum of the moles of *i*-butane, *i*-pentane, *n*-butane, propane, and ethane) vs turnover frequency. It is seen that the tendency to undergo secondary hydrogenolysis is similar for platinum on L- and Y-zeolites, and different for palladium on L-zeolite. Generally, secondary reactions are increased under diffusion-controlled conditions, but the Pd/KL catalysts show less secondary product than the platinum catalysts. This is further evidence against a single-file diffusion effect in L-zeolite for neopentane conversion.

TABLE 5

Partial pressure (kPa)		TOF (total) (s^{-1})		
Hydrogen	Neopentane	Pd/KL (2.0 wt%)	Pt/KL (3.67 wt%, BE)	Pt/KY (3.67 wt%, BE)
6.5	1.00	2.7E-3	2.7E-4	5.9E-4
8.2	1.00	1.3E-3	2.1E-4	3.8E-4
10.4	1.00	5.1E-4	1.8E-4	2.5E-4
12.9	1.00	2.1E-4	1.1E-4	1.4E-4
15.2	1.00	1.1E-4	8.3E-5	9.8E-5
17.5	1.00	7.3E-5	6.0E-5	7.0E-5
10.4	0.57	8.0E-5	5.3E-5	5.8E-5
10.4	0.78	1.0E-4	6.6E-5	7.7E-5
10.4	1.21	1.3E-4	9.2E-5	1.1E-4
10.4	1.43	1.5E-4	1.1E-4	1.3E-4

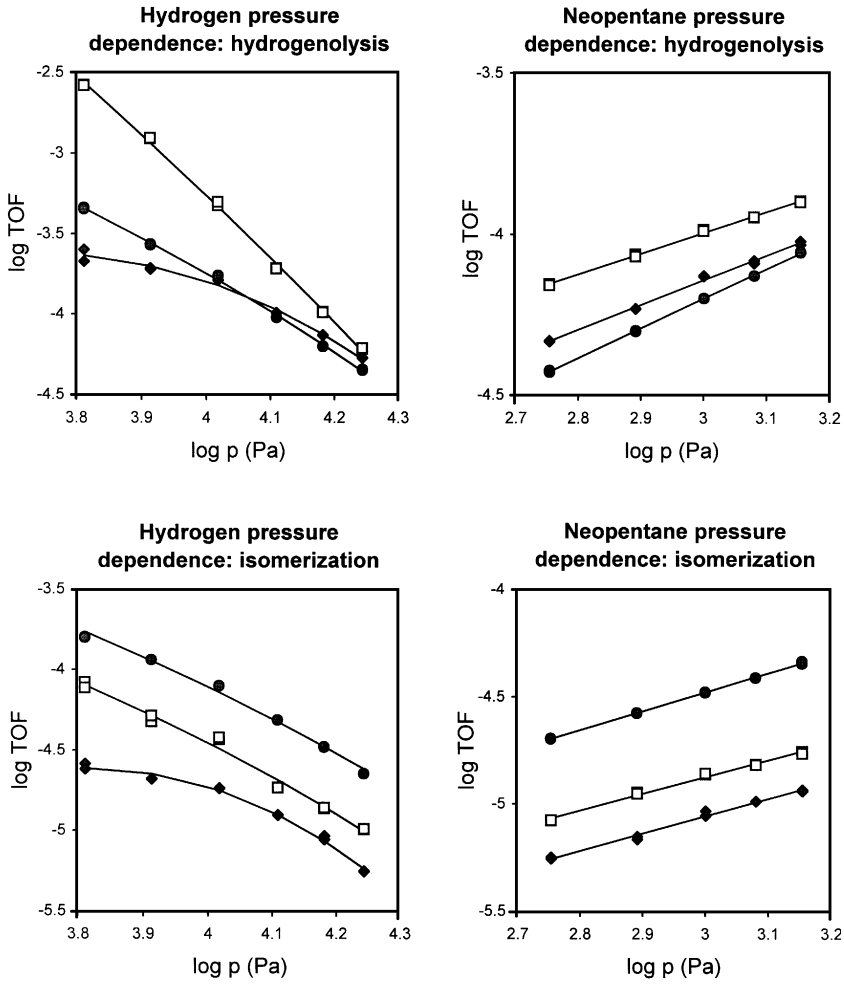

FIG. 7. Partial pressure dependence. (◆) Pt/KL (3.67 wt%, BE), (●) Pt/KY (3.67 wt%, BE), (□) Pd/KL (2.0 wt%).

Reaction Mechanism

The proposed mechanisms for the skeletal rearrangement of hydrocarbons over platinum group metals have been reviewed by Clarke and Rooney (20) and Gault (21). Skeletal rearrangement of neopentane is thought to proceed via a bond shift mechanism. It has been suggested (22) that if bond shift isomerization involves first carbon–carbon bond rupture and then carbon–carbon bond recombination, a common intermediate should exist, leading to both hydrogenolysis and isomerization products. Indeed, we observe the same reaction orders in hydrogen and neopentane partial pressures for hydrogenolysis and isomerization, over platinum supported on KL- and KY-zeolite. Gehrer and Hayek (23), in a study of model thin-film catalysts, observed a relative independence of selectivity toward isomerization on crystallographic orientation and pretreatment, and concluded that both hydrogenolysis and isomerization occur via the same adsorbed state involving a single metal atom. On platinum, the metallacyclobutane intermediate is thought to be formed directly (20, 21), which is then converted to products via olefin metathesis rearrangement. The observed reaction orders of ~ -2 in hydrogen for Pt/KL-zeolite are consistent with the formation of a metallacyclobutane intermediate, using the model proposed by Garin and Gault (24) for hydrocarbon adsorption involving bimolecular dehydrogenation steps, i.e.,

$$C_5H_{12}\ (g) + H\ (a) \leftrightarrow C_5H_{11}\ (a) + H_2\ (g) \qquad [1]$$

$$C_5H_{11}\ (a) + H\ (a) \leftrightarrow C_5H_{10}\ (a) + H_2\ (g). \qquad [2]$$

Therefore,

$$\Theta_{NP} = K_1 \times K_2 \times P_{NP} \times P_{H_2}^{-2} \times \Theta_H^2, \qquad [3]$$

where hydrogen coverage, Θ_H, is practically constant. The slow step is then the conversion of the adsorbed species to products, i.e.,

$$\text{rate} = k \times \Theta_{NP}. \qquad [4]$$

The Pt/KY-zeolite exhibits reaction orders of ~ -2.5 in hydrogen partial pressure for hydrogenolysis and

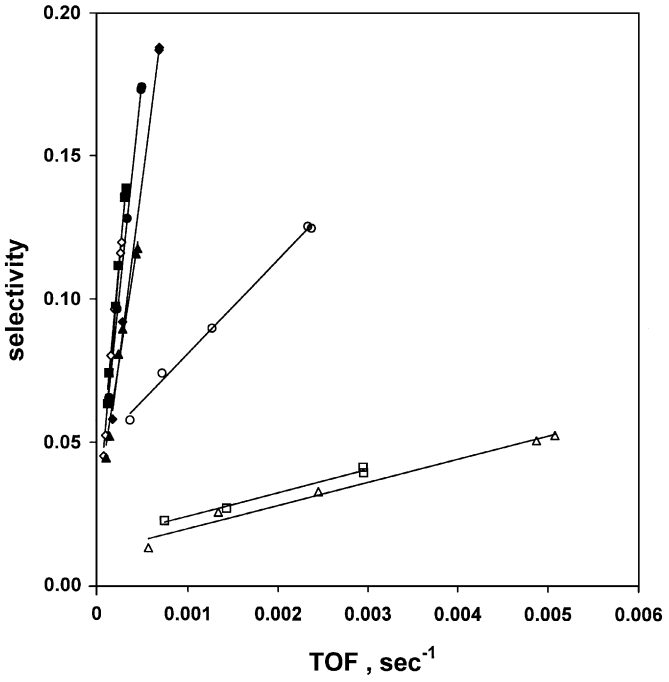

FIG. 8. Selectivity toward secondary (and tertiary) hydrogenolysis vs TOF. (△) Pd/KL (3.0 wt%), (□) Pd/KL (2.0 wt%), (○) Pd/KL (2.0 wt%, BE), (◇) Pt/KL (3.67 wt%), (▲) Pt/KL (3.67 wt%, BE), (■) Pt/BaKL (5.5 wt%), (●) Pt/KY (3.67 wt%), (◆) Pt/KY (3.67 wt%, BE).

isomerization. This suggests that the adsorbed intermediate is more dehydrogenated, possibly involving an additional unimolecular dehydrogenation step, i.e.,

$$C_5H_{10}\ (a) \leftrightarrow C_5H_9\ (a) + H\ (a) \qquad [5]$$

$$H\ (a) + H\ (a) \leftrightarrow H_2\ (g). \qquad [6]$$

Therefore,

$$\Theta_{NP} = K_1 \times K_2 \times P_{NP} \times P_{H_2}^{-2.5} \times \Theta_H^{2.5}. \qquad [7]$$

As is discussed in the next section, since the activation energy increases with the enthalpy of adsorption. The adsorbed species on the Pt/Y-zeolite samples are more dehydrogenated than the adsorbed species on the Pt/L-zeolite samples. This may be the reason that the activation energies for neopentane conversion over the Pt/Y-zeolite samples are larger than those for Pt/L-zeolite samples.

Palladium is unable to promote the direct formation of the metallacyclobutane intermediate. Early work on neopentane conversion over palladium films reported initial isomerization activity which dies off very quickly (25, 26). Since this deactivation was probably caused by sulfur poisoning, this suggests that the isomerization requires an ensemble of more than one metal atom. Since isomerization of neopentane is observed over highly dispersed palladium supported on both Y-zeolite (27) and L-zeolite (7; present work), this suggests that the required ensemble may be as small as two adjacent palladium atoms. The Pd/KL catalyst shows the same orders in reactant partial pressures as the Pt/KL catalyst for the isomerization reaction, i.e., ~ -2 and 0.8 in hydrogen and neopentane, respectively. Therefore the reaction pathway for isomerization probably proceeds via a diadsorbed intermediate state ($\alpha\gamma$ diadsorbed on two adjacent metal centers). The reaction orders for the hydrogenolysis reaction are ~ -4 in hydrogen partial pressure and 0.64 in neopentane partial pressure. The enhanced apparent activation energies for hydrogenolysis are related to the high negative order in hydrogen partial pressure. Correlations between apparent activation energies and the order in hydrogen partial pressure (i.e., the more negative the order in hydrogen, the higher the apparent activation energy) have been observed previously (24, 28) for hydrocarbon reactions over metals. Garin and Gault (24) have reported apparent activation energies of 71 kcal/mol, for *n*-pentane isomerization over a Pt/alumina catalyst, where the observed order in hydrogen partial pressure was -3.4. High negative orders (~ -3.6) in hydrogen partial pressure have been observed previously by Juszczyk and Karpinski (29) for neopentane hydrogenolysis over Pd/silica catalysts. Although the high negative order in hydrogen partial pressure for neopentane hydrogenolysis over Pd/L-zeolite can arise from extensive dehydrogenation of the adsorbed intermediate, this does not explain the decrease in the partial pressure dependence of neopentane. A second possibility, suggested by a comparison of the reaction orders for hydrogenolysis and isomerization, is that the dominant pathway for hydrogenolysis over these catalysts proceeds via a transition state formed from two adsorbed neopentane molecules, i.e.,

$$\text{rate} = k \times \Theta_{NP}^2. \qquad [8]$$

It is now well accepted that the skeletal rearrangement of hydrocarbons can take place through multiple pathways, with a particular pathway dominating under a given set of conditions. Bimolecular reactions have previously been postulated for the isomerization of butanes over sulfated zirconia catalysts (30, 31). Recent work in our lab (14) suggests that the L-zeolite support promotes the formation of a highly specific disc-like morphology of the metal particles. It is possible that in this morphology the neopentane molecules are adsorbed adjacent to each other such that a bimolecular reaction is facilitated. Therefore, the enhanced activation energies observed for these catalysts may be due to a transition state formed from two adsorbed neopentane molecules.

Compensation Effect

A compensation effect for neopentane conversion over supported palladium catalysts has been reported previously by Karpinski *et al.* (7). In the present study, compensation effects are observed for zeolite-supported platinum and

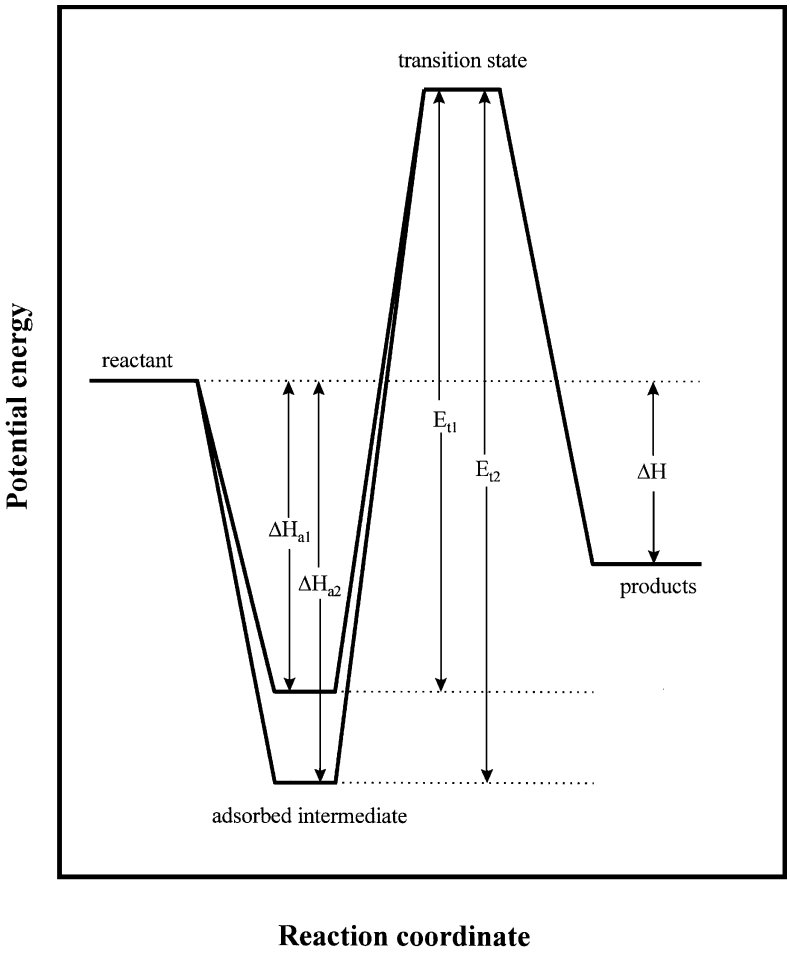

FIG. 9. Reaction pathway.

palladium catalysts. Galwey (32) has reviewed various models proposed to explain compensation effects in heterogeneous catalysis. However, there is still no clear understanding of these phenomena [for more recent reviews, see Bond (34) and Linert *et al.* (35)].

Gault (21) has proposed that since the dehydrogenation steps in the adsorption of alkanes (Eqs. [1], [2], and [5]) are endothermic, the enthalpy changes for the dehydrogenation steps will contribute to the observed activation energies. The following model, based on ideas expressed by Bond in a recent communication (35), can explain the compensation effects observed in the present study. Bond (35) has pointed out that for reactions proceeding via an adsorbed intermediate the enthalpy of adsorption will contribute to the observed activation energy. This is depicted in Fig. 9, where it is seen that different enthalpies of adsorption (ΔH_{a1} and ΔH_{a2}) can lead to different activation energies (E_{t1} and E_{t2}), assuming that both reactions proceed via a similar transition state. If the formation of the adsorbed species is assumed to be at equilibrium (Eqs. [1], [2], and [5]), then for the case of the unimolecular rearrangement of an adsorbed molecule (Eq. [4]),

$$\text{rate} = k \times \Theta_{NP} = A \times \exp(-E_t/RT) \times \Theta_{NP}. \quad [9]$$

The concentration of the adsorbed intermediate can be related to the enthalpy of adsorption by the vant Hoff relationship, i.e.,

$$\Delta G_a = \Delta H_a - T\Delta S_a = RT \ln(K_c). \quad [10]$$

From Eqs. [9] and [10], we get

$$\text{rate} = \{A \times \exp(\Delta S/R)\} \times \{\exp((-E_t + \Delta H_a)/RT)\} \times \Theta_{NP}. \quad [11]$$

Therefore, as pointed out by Bond (35), the enthalpy of adsorption contributes twice to the apparent activation energies observed, both in the magnitude of E_t and in the effect on the equilibrium concentration of the adsorbed species at the reaction temperature. If the free energy changes upon adsorption (ΔG_a) are similar over the

different catalysts, then the larger the enthalpy changes upon adsorption (ΔH_a) the larger the entropy difference (ΔS_a), which contributes to the preexponential factor as shown in Eq. [11]. Therefore an increase in the apparent activation energy will be compensated by an increase in the preexponential factor, leading to a compensation effect.

Electronic Modification of the Metal Particles

Platinum and palladium supported on KL-zeolite have similar activation energies and preexponential factors for the high and low loadings, respectively. However, back exchanging for the protons with K^+ had a big effect on these parameters for the platinum and palladium catalysts. Figure 10 shows the infrared absorption in the hydroxyl stretching region for the different samples (36). From this it is seen that the back exchange is successful in removing all of the Brønsted acidity (at ~3746 cm^{-1}) generated in the ion-exchange preparation. The Pt/KL- and Pt/KY-zeolite samples and the Pd/KL-zeolite samples show opposite trends in the amount of hydrogen chemisorbed with variation in Brønsted acidity. A comparison of the chemisorption and TPD of hydrogen for the ion-exchanged samples and their back-exchanged counterparts indicates that for the platinum catalysts, back-exchange results in a greater fraction of higher binding energy states for hydrogen and less total uptake of hydrogen, while the reverse trend is observed for the palladium catalysts. Figure 11 shows the normalized EXAFS chi functions for the ion-exchanged and back-exchanged catalysts (15). This indicates that there is negligible effect of the back exchange on the metal particle size and/or distribution, and that the changes in activation energies and hydrogen chemisorption are due to an electronic modification of the metal particles by the interaction with the support. The decreased chemisorption of hydrogen for palladium catalysts in the presence of Brønsted acidity has been reported previously by Xu *et al.* (37).

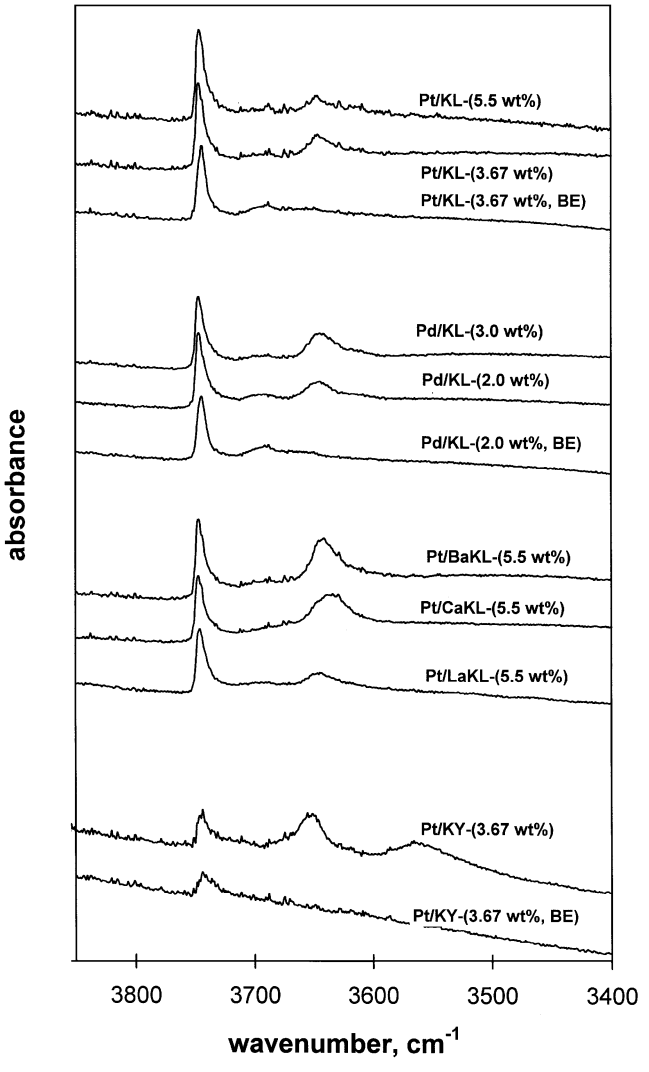

FIG. 10. Infrared absorption in hydroxyl stretching region.

A qualitative trend (because particle size effects cannot be completely excluded) in the TPD of hydrogen can also be observed in the Pt/L-zeolite (5.5 wt%) samples, where the total desorption of hydrogen changes with the exchanged cation. For the 5.5 wt% platinum samples on L-zeolite, the activation energies and preexponential factors are similar for the Pt/KL- and Pt/LaKL samples, and for the Pt/BaKL and Pt/CaKL samples. From Fig. 10, it can be seen that the Brønsted acid peak positions are similar for the Pt/KL and Pt/LaKL samples, and for the Pt/CaKL and Pt/BaKL samples. It has been observed previously (38) that upon calcination, Ba^{2+} and Ca^{2+} have a much higher occupation of site B positions (located at the center of the cancrinite cage) than La^{3+}, which preferentially populates site A positions (located at the center of the hexagonal prism). The similar activity of Pt/KL and Pt/LaKL-zeolites may be related to the low occupation of the site B positions by the La^{3+} ions, i.e., it appears that the cations present in the site B positions may be responsible for the lower Brønsted acid hydroxyl stretching frequencies and the lower activation energies over the Pt/CaKL- and Pt/BaKL-zeolite samples.

It is observed that the greater the fraction of higher binding energy states of hydrogen for a set of similar catalysts (or alternatively, the less the hydrogen uptake), the higher the observed apparent activation energy. This is in agreement with the proposed model, since an increase in the binding energy for hydrogen would increase the endothermicity of the dehydrogenation steps. Therefore, it appears that the difference in activation energies reflects the electronic perturbation of the metal particles by the support, and the resulting change in the enthalpy of adsorption of the reactants.

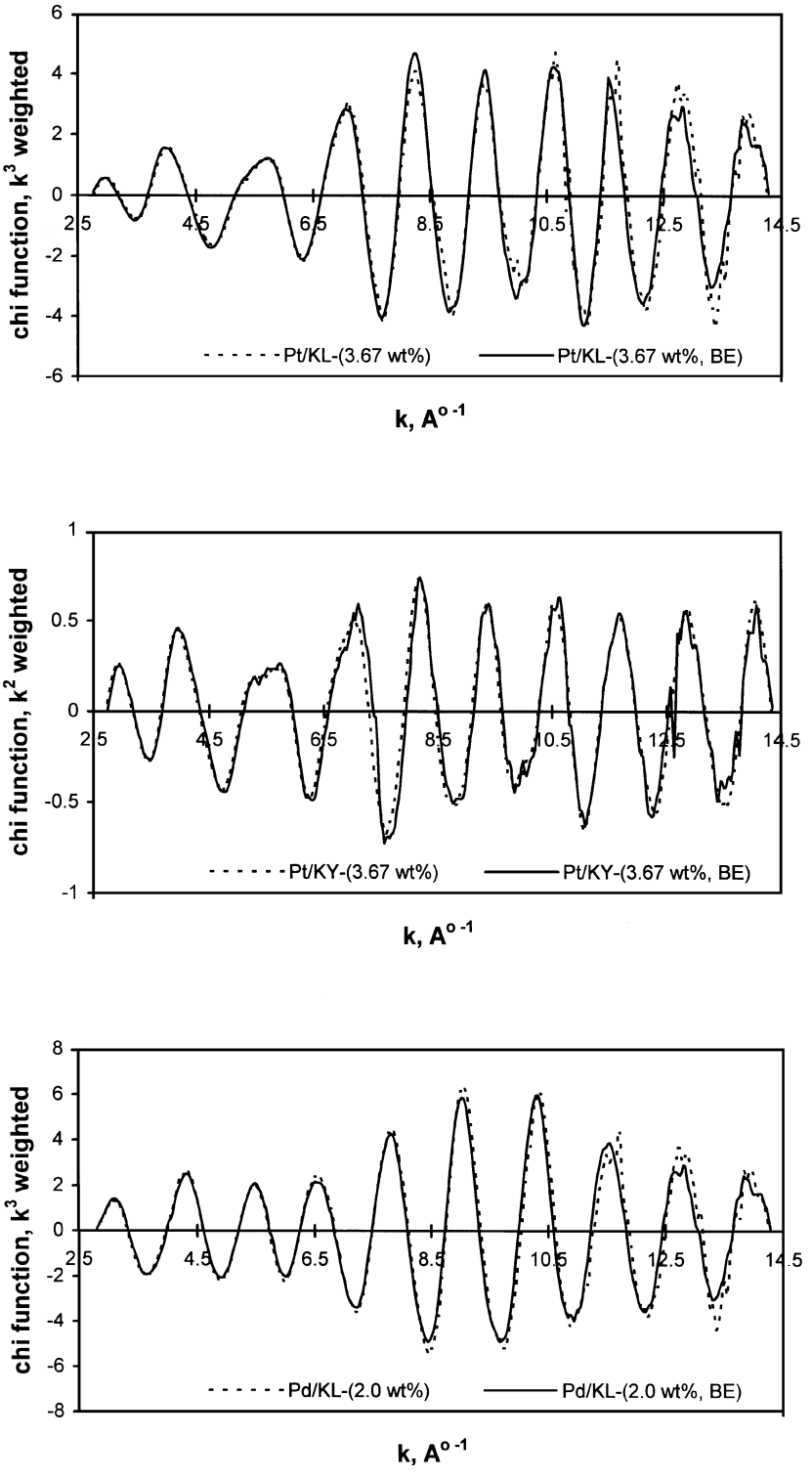

FIG. 11. EXAFS data (14).

CONCLUSION

Neopentane conversion has been studied over platinum supported on L- and Y-zeolites, and palladium supported on KL-zeolite. It is concluded that the neopentane conversion, under the conditions of the temperature-dependence studies, is not diffusion limited. The reaction orders in hydrogen and neopentane are in agreement with a

metallacyclobutane (α,γ-diadsorbed) adsorption intermediate for neopentane conversion over the platinum catalysts. Activation energies for Pt/L-zeolites are smaller than those for Pt/Y-zeolites. This may be due at least partly to a greater degree of dehydrogenation of the adsorbed intermediate over the latter. Neopentane hydrogenolysis over Pd/L-zeolites, which display enhanced activation energies (75–80 kcal/mol) and very high negative orders in hydrogen (~ -4), are proposed to be due to a reaction pathway involving two adsorbed neopentane molecules. Compensation effects are observed for the hydrogenolysis and isomerization of neopentane over the palladium and platinum catalysts. Over a set of similar catalysts, activation energies increase with increase in the binding energy of hydrogen. This is attributed to electronic modification of the metal particles by the interaction with protons and/or charge-compensating cations. Pd/L-zeolites show the opposite trend of Pt/L-zeolites in the variation of activation energies with Brønsted acidity and cation exchange. However, since reaction temperatures are well above the isokinetic temperatures for Pd/L-zeolite, they show the same trend in activity.

ACKNOWLEDGMENTS

P.V.M thanks Dr. Marcos Fernandez-Garcia for helpful discussions. This work was supported by a research grant from NSF.

REFERENCES

1. Chen, N. Y., and Weisz, P. B., *Chem. Eng. Progr. Symp. Ser.* **63**(73), 86 (1967).
2. Homeyer, S. T., Karpinski, Z., and Sachtler, W. M. H., *J. Catal.* **123**, 60 (1990).
3. Modica, F. S., Miller, J. T., Meyers, B. L., and Koningsberger, D. C., *Catal. Today* **21**, 37 (1994).
4. Mojet, B. L., Kappers, M. J., Muisjers, J. C., Niemantsverdriet, J. W., Miller, J. T., Modica, F. S., and Koningsberger, D. C., *Stud. Surf. Sci. Catal.* **84**, 909 (1994).
5. Foger, K., and Anderson, J. R., *J. Catal.* **54**, 318 (1978).
6. Bai, X., Zhang, Z., and Sachtler, W. M. H., *Appl. Catal.* **72**, 165 (1991).
7. Karpinski, Z., Gandhi, S. N., and Sachtler, W. M. H., *J. Catal.* **141**, 337 (1993).
8. Stakheev, A. Y., and Sachtler, W. M. H., *Catal. Today* **12**, 28 (1992).
9. Besoukhanova, C., Guidot, J., Barthomeuf, D., Breysse, M., and Bernard, J. R., *J. Chem. Soc. Faraday Trans. I* **77**, 1595 (1981).
10. Larsen, G., and Haller, G. L., *Catal. Today* **15**, 431 (1992).
11. Newell, P. A., and Rees, L. V. C., *Zeolites* **3**, 21 (1983).
12. Larsen, G., Ph.D. Dissertation, Yale University, 1993.
13. Press, W. H., Teukolsky, S. A., Vetterling, W. T., and Flannery, B. P., "Numerical Recipes in C," 2nd ed., p. 650. Cambridge Univ. Press, Cambridge, UK, 1992.
14. Menacherry, P. V., Fernandez-Garcia, M., and Haller, G. L., *J. Catal.* **166**, 75 (1997).
15. Menacherry, P. V., Fernandez-Garcia, M., and Haller, G. L., unpublished results.
16. Bhore, N. T., Klein, M. T., and Bischoff, K. B., *Ind. Eng. Chem. Res.* **29**, 313 (1990).
17. Koros, R. M., and Nowak, E. J., *Chem. Eng. Sci.* **22**, 470 (1967).
18. Satterfield, C. N., "Mass Transport in Heterogeneous Catalysis," p. 12. M. I. T. Press, Cambridge, MA, 1970.
19. Karger, J., Petzold, M., Pfeifer, H., Ernst, S., and Weitkamp, J., *J. Catal.* **136**, 283 (1992).
20. Clarke, J. K. A., and Rooney, J. J., *Adv. Catal.* **25**, 125 (1976).
21. Gault, F. G., *Adv. Catal.* **30**, 1 (1981).
22. Barron, Y., Maire, G., Muller, J. M., and Gault, F. G., *J. Catal.* **24**, 385 (1972).
23. Gehrer, E., and Hayek, K., *J. Mol. Catal.* **39**, 293 (1987).
24. Garin, F., and Gault, F. G., *J. Am. Chem. Soc.* **97**, 4466 (1975).
25. Karpinski, Z., and Koscielski, T., *J. Catal.* **56**, 430 (1979).
26. O'Donohoe, C., Clarke, J. K. A., and Rooney, J. J., *J. Chem. Soc. Faraday Trans. I* **76**, 345 (1980).
27. Homeyer, S. T., Karpinski, Z., and Sachtler, W. M. H., *Recl. Trav. Chim. Pays-Bas* **109**, 81 (1990).
28. Sinfelt, J. H., Taylor, W. F., and Yates, D. J. C., *J. Phys. Chem.* **69**, 95 (1965).
29. Juszczyk, W., and Karpinski, Z., *React. Kinet. Catal. Lett.* **37**, 367 (1988).
30. Zarkalis, A. S., Hsu, C.-Y., and Gates, B. C., *Catal. Lett.* **29**, 235 (1994).
31. Adeeva, V., Lei, G. D., and Sachtler, W. M. H., *Catal. Lett.* **33**, 135 (1995).
32. Galwey, A. K., *Adv. Catal.* **26**, 247 (1977).
33. Bond, G. C., *Zeit. Phys. Cem. N. F.* **144**, 21 (1985).
34. Linert, W., and Jameson, R. F., *Chem. Soc. Rev.* **18**, 477 (1989).
35. Bond, G. C., *Catal. Today* **17**, 399 (1993).
36. Menacherry, P. V., and Haller, G. L., unpublished results.
37. Xu, L., Zhang, Z., and Sachtler, W. M. H., *J. Chem. Soc. Faraday Trans.* **88**(15), 2291 (1992).
38. Newell, P. A., and Rees, L. V. C., *Zeolites* **3**, 28 (1983).